Free Radical Research, January 2007; 41(1): 89–96

informa
healthcare

Induction of oxidative cell damage by photo-treatment with zinc *meta N*-methylpyridylporphyrin

DALAL A. AL-MUTAIRI[1,†], JAMES D. CRAIK[1], INES BATINIC-HABERLE[2], & LUDMIL T. BENOV[1]

[1]*Department of Biochemistry, Faculty of Medicine, Kuwait University, Safat, Kuwait, and* [2]*Department of Radiation Oncology, Duke University Medical Center, Durham, NC 27710, USA*

Accepted by Professor M. Davies

(Received 21 May 2006)

Abstract

We have previously reported that isomeric Zn(II) *N*-methylpyridylporphyrins (ZnTM-2(3,4)-PyP^{4+}) can act as photosensitizers with efficacy comparable to that of hematoporphyrin derivative (HpD) in preventing cell proliferation and causing cell death *in vitro*. To better understand the biochemical basis of this activity, the effects of photo-activated ZnTM-3-PyP^{4+} on GSH/GSSG ratio, lipid peroxidation, membrane permeability, oxidative DNA damage, and the activities of SOD, catalase, glutathione reductase, and glutathione peroxidase were evaluated. Light exposure of ZnTM-3-PyP^{4+}-treated colon adenocarcinoma cells caused a wide spectrum of oxidative damage including depletion of GSH, inactivation of glutathione reductase and glutathione peroxidase, oxidative DNA damage and peroxidation of membrane lipids. Cell staining with Hoechst-33342 showed morphological changes consistent with both necrotic and apoptotic death sequences, depending upon the presence of oxygen.

Keywords: *Photodynamic therapy, Zn* meta N-*methylpyridylporphyrin, oxidative stress, lipid peroxidation, cell death*

Abbreviations: *ZnTM-3-PyP^{4+},* meta isomer*, Zn(II) tetrakis(N-methylpyridinium-3-yl)porphyrin; PDT, photodynamic therapy; HpD, hematoporphyrin derivative; SOD, superoxide dismutase; MDA, malondialdehyde; 8-OHdG, 8-hydroxy-2′-deoxyguanosine; ROS, reactive oxygen species; RNS, reactive nitrogen species; ANOVA, analysis of variance*

Introduction

Lipid peroxidation is a major consequence of oxidative stress [1,2] and is involved in the mechanism of some current treatments of cancer, including photodynamic therapy (PDT) [3–7]. In PDT, oxygen, light, and photosensitizers are used in combination to kill tumor cells [8]. Photosensitizers are compounds that absorb energy from light at specific wavelengths and use this energy to induce reactions in other, non-absorbing molecules. The photodynamic reactions start with absorption of a photon by the photosensitizer converting it to excited state [3]. There are two types of photodynamic reactions [9]. Type I reactions involve electron or hydrogen transfer reactions between first excited triplet state (T_1) of the photosensitizers and other molecules which produce reactive intermediates that are harmful to the cells, such as superoxide, hydroperoxyl radical, hydroxyl radical, and hydrogen peroxide. These types of

Correspondence: L. Benov, Department of Biochemistry, Faculty of Medicine, Kuwait University, P. O. Box 24923, Safat 13110, Kuwait. Tel: 965 531 9489. Fax: 965 533 8908. E-mail: lbenov@hsc.edu.kw

[†]This work forms part of a MSc thesis submission by Dalal Al-Mutairi to the College of Graduate Studies, Kuwait University (Supervisor L. Benov and co-supervisor J. Craik).

ISSN 1071-5762 print/ISSN 1029-2470 online © 2007 Informa UK Ltd.
DOI: 10.1080/10715760600952869

reactions result in photo-oxidations by free radicals [8]. The type II photoprocess is an electron spin exchange between (T_1) photosensitizers and molecular oxygen ($^3O_2$), which produces the cytotoxic excited singlet state of oxygen ($^1O_2$). The lifetime of $^1O_2$ in the cellular environment is short and, therefore, it reacts in the immediate vicinity of its site of formation. Singlet oxygen ($^1O_2$) is considered to be the principal mediator of phototoxicity in PDT. It is a powerful oxidant that can react with many types of biomolecules, including lipids, proteins, and nucleic acids [2]. Therefore, both Type I and II photodynamic reactions can induce oxidative stress. They can operate simultaneously and the relative importance of these two mechanisms in a cellular system depends on sensitizer localization, the concentration of oxygen, the target molecule, and efficacy of energy transfer from the sensitizer to oxygen [2,3].

Porphyrins, developed as photosensitizers in the 1970s and early 1980s, represent the first generation of PDT agents. The chemical nature of porphyrins permits a wide variety of chemical modifications that may influence the biological and photochemical properties of the resulting derivatives. In particular, sensitivity to longer wavelengths of light could increase the applicability of PDT to target cells deeper within the tissues, while more selective cellular uptake, or more rapid clearance from the body, would decrease undesirable non-specific photosensitivity reactions.

We have reported previously that Zn *N*-methylpyridylporphyrins are powerful photosensitizers [10,11] with activities comparable to hematoporphyrin D in causing cell death and preventing the proliferation of human colon adenocarcinoma cells *in vitro* [11]. This study was undertaken to investigate the possible role of oxidative stress in ZnTMPyP-induced cell damage. Since no great differences among the ZnTMPyP isomers (charges are omitted throughout text) were observed with respect to cell killing [11], we selected the *meta* isomer (Zn(II) tetrakis(*N*-methylpyridinium3-yl)porphyrin (ZnTM-3-PyP)) (Figure 1) as a typical representative of this family of compounds and investigated its ability to induce oxidative damage in human colon carcinoma LS174T cells.

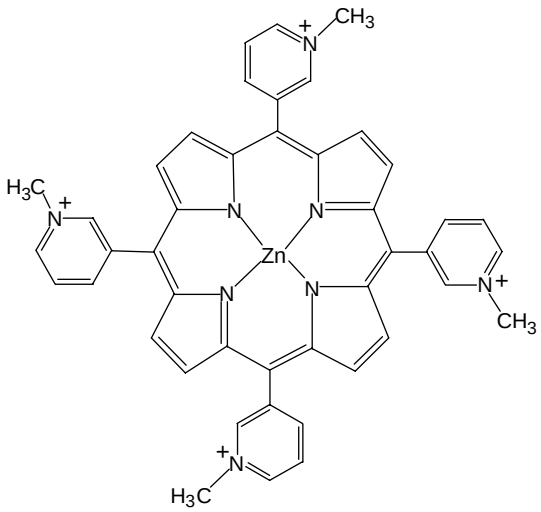

Figure 1. Structure of the *meta* isomer of ZnTM-3-PyP.

Materials and methods

Cells, photosensitizers and illumination

The ZnTM-3-PyP was prepared as described previously [10].

The human colon adenocarcinoma LS174T cell line was kindly provided by Dr Christopher Ford (Faculty of Medicine, Kuwait University). The cells were grown in minimal essential medium (MEM), (Gibco BRL) supplemented with 10% fetal bovine serum, 1.2% L-glutamine, 1.2% MEM nonessential amino acids, and 1.2% penicillin/streptomycin. Cells were incubated at 37°C under 5% CO_2 saturation and were used for experiments at ~80–90% confluence. Sterile solutions of the photosensitizer were added giving a concentration of 20 μM, 30 min prior to illumination of the plates. Two TL8W Philips white fluorescent tubes mounted on a light box beneath a white translucent screen provided a fluence rate of 0.5 mW/cm^2 and were used in all photo-activation protocols. No measurable increase of the temperature was observed during the periods of illumination. The controls (non-illuminated, non-treated), the light controls (illumination without photosensitizers) and dark controls (containing the same concentration of the photosensitizer, but kept in the dark) were analyzed in parallel with experimental samples. Since no differences between the non-treated, non-illuminated controls, and non-treated but illuminated controls were observed, only results for the light controls are presented. Treatment conditions with respect to photosensitizer concentrations and illumination times were based upon those already shown to have cytotoxic effects using this cultured cell system [11].

Hypoxia

In order to investigate the effects of hypoxia on photodynamic activities, 96- or 6-well plates with ~80–90% confluent cells were first preincubated in the dark with ZnTM-3-PyP for 30 min. The plates were then transferred into transparent plastic bags, purged three times with argon, left for 15 min to permit gas equilibration, and illuminated under argon. All manipulations were undertaken in a dark room.

Estimation of aldehyde products of lipid peroxidation

Lipid peroxidation was assessed by measuring short chain aldehydes, which are among the major toxic aldehydes produced by oxidative damage [12].

Aldehydes were determined as described by Steghens et al. [13]. The assay is based on the derivatization of aldehydes with diamionaphtalene to give characteristic diazepinium adducts in an acidic medium at 37°C followed by HPLC analysis (C18 reversed phase column). A Shimadzu 10ADM VP HPLC system equipped with CLASS-VP Chromatography data software was used. Identification of the peaks was performed by comparing their retention times and spectra with those of the corresponding standards.

Reduced and oxidized glutathione

The GSH/GSSG ratio was measured using a Bioxytech GSH/GSSG-412 kit (Oxis International Inc., Portland, OR, USA) following the manufacturer's instructions. The GSH/GSSG assay uses the thiol-scavenging reagent, 1-methyl-2-vinylpyridinium trifluoromethanesulfonate to trap GSH. To avoid GSH oxidation during sample handling, the adherent cells were scraped away from the plastic surface of the culture flask with a rubber policeman, rapidly centrifuged and briefly washed with 1.0 ml cold PBS. All procedures were done in a cold room and centrifuge tubes were kept on ice. The cell pellet was used directly for the assay without sonication.

Enzymes

The following enzyme activities were assayed in freshly prepared cell-free extracts: aconitase [14,15]; SOD [16]; catalase [17]; glutathione reductase [18]; and glutathione peroxidase (using a commercial Glutathione Peroxidase assay kit, Oxis International Inc., Portland, OR, USA). Control samples (no photosensitizer present in medium added to cells), cells treated with the porphyrin in the dark, and cells treated with the porphyrin and illuminated were washed with 5.0 ml of PBS, and aliquots were resuspended in respective buffers for the enzyme assays. The cells were sonicated on ice for five cycles (each cycle had 5 s sonication and 10 s rest between cycles). For the aconitase assay, cell disruption was performed as described by Gardner et al. [15].

Oxidative DNA damage

Oxidative DNA damage was assessed by measuring the production of 8-hydroxy-2′-deoxyguanosine (8-OHdG). 8-OHdG was assayed with Bioxytech 8-OHdG-EIA kit (Oxis Health Products Inc., Portland, OR, USA) following the manufacturer's instructions. The kit is based on a competitive enzyme-linked immunosorbent assay (ELISA) for quantitative measurement of 8-OHdG.

Fluorescent staining of nuclei

Morphological changes of nuclei were visualized by staining with a DNA-binding fluorochrome bis-benzimide (Hoechst-33342; Sigma), according to a procedure [19] adapted by Alkhalaf[‡]. Cells were cultured in 6-well plates and treated with 20 μM of ZnTM-3-PyP prior to illumination for 30 min, and the incubation medium was replaced. At the indicated times the medium was removed. Cells were then fixed with methanol–acetic acid 3:1 (v/v) for 10 min (2 ml in each well). Cells were washed with PBS to remove the fixative and then stained by adding 1 ml of 1 μg/ml Hoechst 33342 to each well for 15 min at 37°C in the dark. After 15 min of staining, cells were washed with cold PBS to clear the background. Then, a few drops of the mounting medium (0.466 g of citric acid and 0.778 g of disodium orthophosphate dissolved in 50 ml of distilled water added to 50 ml of glycerol) was added to each well and covered with cover slips. Wells were examined by fluorescence microscopy and photographed (Olympus Bx 51 camera equipped with computerized imaging system using IF550 filter).

All experiments were repeated at least three times with 3–5 replicates. The mean ± SEM are presented. Statistical analysis was performed using ANOVA. $p < 0.005$ was considered statistically significant.

Results

Reduced glutathione

Reduced glutathione plays a major role in cellular defenses against oxidative stress [2,20]. Normally the GSH/GSSG ratio is kept high by the glutathione reductase system. However, if the stress level exceeds the capacity of the cell to reduce GSSG, or other factors limit the GSSG reductase reaction, then GSSG may accumulate [21]. Therefore, GSH/GSSG ratio is a useful indicator of oxidative stress. To investigate this parameter, LS174T adherent cells were preincubated for 30 min with 20 μM ZnTM-3-PyP in the dark and were then illuminated for 30 min. The GSH/GSSG ratio was determined from analysis performed immediately after the illumination. For control cells a ratio of 60 ± 4 was found, while in illuminated cells the ratio was dramatically lowered, 9 ± 2 (mean ± SEM, $n = 3$). This difference was highly significant ($p < 0.005$). No change of the GSH/GSSG ratio was observed in the cells treated with ZnTM-3-PyP but kept in the dark, or in cells illuminated in the absence of the photosensitizer.

Lipid peroxidation

Lipid peroxidation is a destructive process that affects cell membranes and other lipid-containing structures under conditions of oxidative stress [22–24]. It can be induced by free radicals and $^1O_2$ generated through photodynamic action [25]. Figure 2 shows that cellular MDA content was significantly elevated immediately

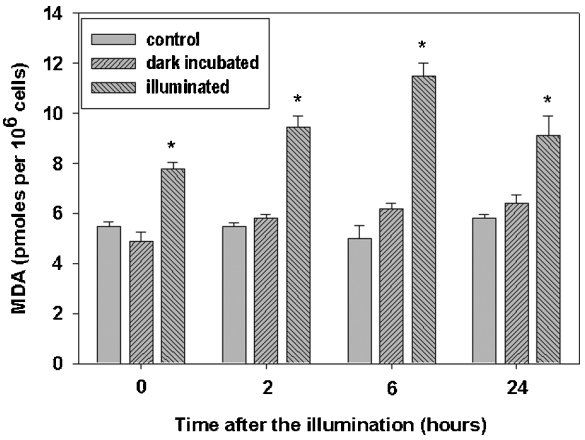

Figure 2. Induction of lipid peroxidation by photoactivated ZnTM-3-PyP. After 30 min preincubation with or without 20 μM ZnTM-3-PyP the cells were either illuminated for 30 min or were kept in the dark (dark incubated). All flasks were kept in a CO_2 incubator for the indicated time intervals. For the MDA assay, the medium was removed and cells were harvested and briefly washed with cold PBS. Derivatization and HPLC analysis were performed as described in the Materials and Methods section. Data are presented as mean ± SEM ($n = 3$).

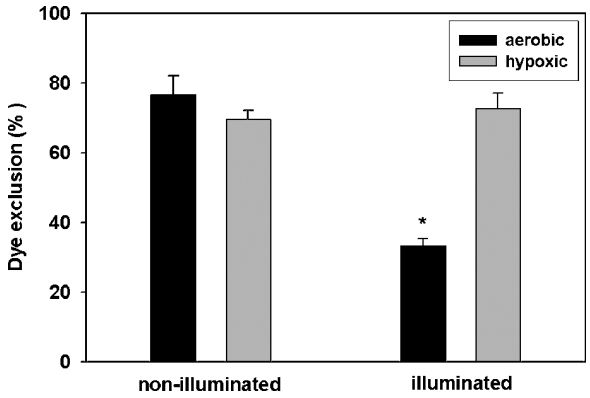

Figure 3. ZnTM-3-PyP-induced plasma membrane permeability changes. Membrane permeability was assessed by trypan blue dye exclusion. Plates (96-well) with ~80% confluent cells were preincubated 30 min with or without 20 μM ZnTM-3-PyP in the dark. To create hypoxic conditions, plates were transferred into transparent plastic bags, purged three times with argon, left for 15 min to permit gas equilibration, and illuminated under argon. After that half of the hypoxic and half of the normoxic plates were illuminated for 30 min, and the rest kept as dark controls. After 6 h in a CO_2 incubator the cells were trypsinized and stained. Stained and non-stained cells were counted under a microscope. Results (mean ± SEM, $n = 5$) are presented as a percentage of the non-stained cells out of the total number of cells.

after the illumination of the cells in the presence of ZnTMP-3-PyP and that it rose continuously in a time-dependent manner, reaching a maximum 6 h after illumination. Similar patterns were observed for acetaldehyde and formaldehyde (not shown). This aldehyde production is clearly the result of illumination, since no comparable increase was observed in the ZnTMP-3-PyP-treated cells in the absence of illumination. Figure 2 also shows that aldehyde production continues long after the end of the illumination. This indicates that once initiated, the oxidative process cannot be controlled by the cellular antioxidant system, which has been compromised by PDT.

Membrane permeability

Peroxidation of membrane lipids is known to disrupt membrane structure. To test the effect of PDT with ZnTM-3-PyP on membrane integrity we examined trypan blue exclusion from cells after photosensitization. Illumination of cells in the presence of ZnTMPyP causes a dramatic increase of the cell membrane permeability (Figure 3). Since no effect on membrane permeability was observed when the cells were incubated with ZnTM-3-PyP in the dark, this is a clear indication that PDT with ZnTM-3-PyP causes plasma membrane disruption. To determine if membrane disruption is a consequence of oxygen-mediated damage, the experiment was repeated with illumination performed on cells equilibrated under an argon atmosphere. The results shown in Figure 3 indicate that oxygen is a crucial factor for ZnTM-3-PyP-induced loss of membrane integrity.

Oxidative DNA damage

DNA is highly susceptible to the oxidative damage because it efficiently binds metals that are involved in the Fenton reaction [9]. 8-OHdG is a useful stable marker of oxidative DNA damage that can be formed by attack of hydroxyl radical and singlet oxygen upon DNA, and by DNA interaction with alkoxyl and peroxyl radicals [1,2]. Illumination of LS147T cells in the presence of ZnTM-3-PyP resulted in a marked and prolonged production of 8-OHdG (Figure 4). Figure 4 also demonstrates that ZnTM-3-PyP did not

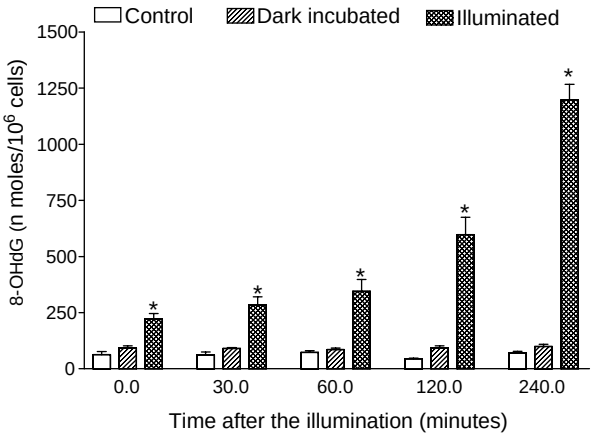

Figure 4. Oxidative DNA damage. All conditions were as described in Figure 2. At the indicated times after the illumination cells were trypsinized, briefly washed with cold PBS, and disrupted for the 8-OHdG assay. Mean ± SEM is presented ($n = 3$).

cause any 8-OHdG production in the absence of light, showing that this oxidative damage to DNA is a completely light-dependent phenomenon.

Antioxidant enzymes

Oxidative stress occurs when the rate of ROS and RNS production exceeds the ability of a system to neutralize and eliminate them to re-establish homeostasis [2,26]. Since activity of antioxidant enzymes can prevent or delay the onset of oxidative damage, and considering that ZnTM-3-PyP might induce enzyme inactivation through photo-damage of proteins, we assayed the activities of SOD, catalase, glutathione reductase, and glutathione peroxidase in the cultured cancer cells in the presence and absence of the porphyrin and illumination.

SOD and catalase

Illumination of cells in the presence of ZnTM-3-PyP did not affect the activities of SOD and catalase (data not shown). This result supports the view that superoxide dismutases are insensitive to photoinactivation [27].

It is well established that cells can respond to increased superoxide production by up-regulation of synthesis of antioxidant enzymes over short time scales [28]. Since SOD is responsible for scavenging of $O_2^{\cdot -}$, the lack of change in SOD activity might indicate that formation of superoxide by type I reactions does not play a major role in ZnTM-3-PyP-induced oxidative stress. To further explore this possibility, we also assessed the activity of aconitase as an indicator for intracellular superoxide production. Aconitase is an iron–sulfur-containing dehydratase which is sensitive to inactivation by superoxide anion and whose activity is modulated by changes in $O_2^{\cdot -}$ levels in cells [14–15]. Aconitase activity was not significantly altered in control cells (no porphyrin treatment), ZnTM-3-PyP-treated cells in the dark, and ZnTM-3-PyP-treated and illuminated cells (data not shown), a result that supports a conclusion that photo-excitation of ZnTM-3-PyP does not lead to markedly increased intracellular production of superoxide.

Glutathione reductase and glutathione peroxidase

In contrast to SOD and catalase, glutathione reductase (Figure 5) and glutathione peroxidase (Figure 6) activities were almost completely terminated by photo-activation of ZnTM-3-PyP. The inactivation of both enzymes occurred during the period of illumination and no further changes were observed when, after the completion of the illumination, cells were incubated for an additional 4 h in the dark. The lack of recovery of the enzymes during the incubation after the illumination suggests that both enzymes were irreversibly damaged and were not replaced by *de novo* protein synthesis over this timescale. Neither glutathione reductase nor glutathione peroxidase activity were affected if the cells were treated with ZnTM-3-PyP, but incubated in the dark.

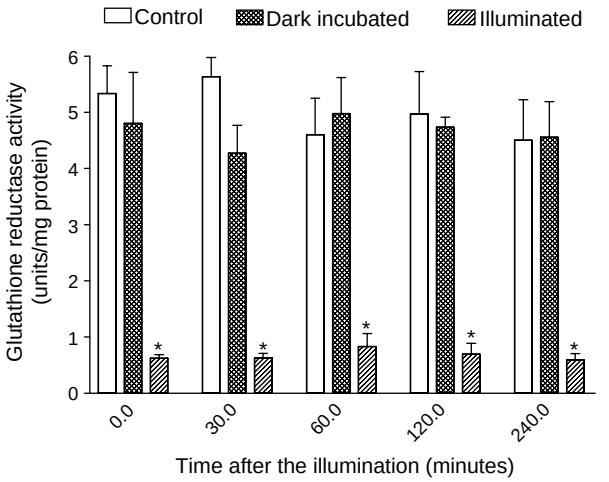

Figure 5. Glutathione reductase activity. All conditions were as described in Figure 2. At the indicated times the medium was removed, the adherent cells were harvested, briefly washed with cold PBS, resuspended in the assay buffer and disrupted by sonication. Mean ± SEM is presented ($n = 3$).

Nuclear morphological alterations induced by the photodynamic treatment

PDT can cause cell death by apoptosis or necrosis [29]. To investigate the mode of killing, we followed Hoechst-33342 staining of cells that were illuminated in the presence and absence of the photosensitizer, as well as of cells treated with ZnTM-3-PyP in the dark. Typically, Hoechst staining is weak in normal nuclei, strong and uniform in necrotic nuclei, and strong in condensed zones in apoptotic nuclei [30]. Figure 7, panels (a) and (b) show normal, non-treated cells 2

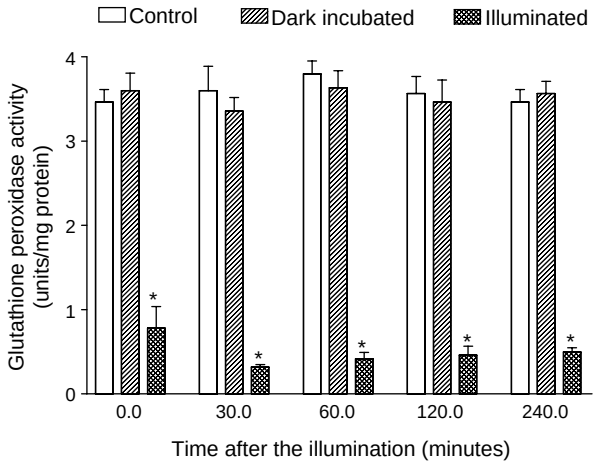

Figure 6. Glutathione peroxidase activity. All manipulations except the activity assay were performed as described in Figure 5.

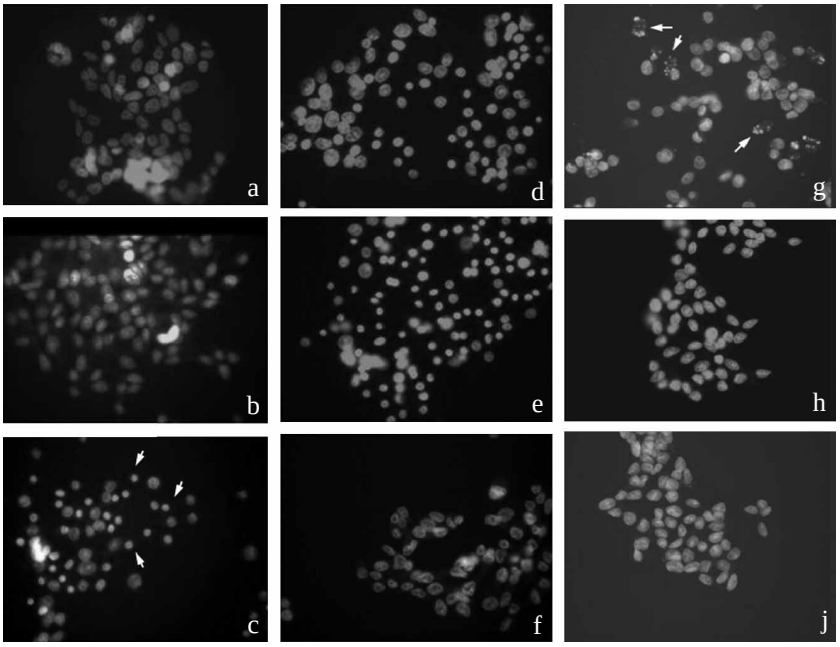

Figure 7. Fluorescence images of Hoechst 33342-stained LS147T cells. Panels: (a) control, non-treated cells 2 h after the illumination; (b) the same cells 24 h after the illumination; (c) cell illuminated in the presence of ZnTM-3-PyP, 2 h after the illumination; (d) cell illuminated in the presence of ZnTM-3-PyP, 6 h after the illumination; (e) cell illuminated in the presence of ZnTM-3-PyP, 24 h after the illumination; (f) cell incubated with ZnTM-3-PyP and kept in the dark for 24 h; (g) cell illuminated under argon in the presence of ZnTM-3-PyP, 24 h after the illumination; (h) cells illuminated under hypoxic conditions without being treated with ZnTM-3-PyP, and (j) cells treated with ZnTM-3-PyP under argon and incubated in the dark.

and 24 h after the illumination, respectively. The illumination protocol produced no observable changes when compared to cells kept in the dark (results not shown). Two hours after the illumination in the presence of ZnTM-3-PyP (panel (c)) about half of the cells demonstrate shrunken, brightly stained nuclei (arrows), a feature typical of necrosis. At 6 h after the illumination the shrinking of the nuclei has progressed (panel (d)), and at 24 h after the illumination very few cells show normal morphology (panel (e)). Cells treated with ZnTM-3-PyP in the dark (panel (f)) remained unaltered when incubated for 24 h with ZnTM-3-PyP.

The nuclear morphological changes depicted on Figure 7 (panels (c)–(e)) suggest that necrosis is an important mechanism of ZnTM-3-PyP-induced cell death. To determine if it is primarily a consequence of photo-induced oxidative stress, the cells were illuminated under an argon atmosphere. Respective non-treated controls and ZnTM-3-PyP-treated cells kept in the dark were placed under argon in identical conditions. After illumination the cells were maintained in a CO_2 incubator under aerobic conditions exactly as for the aerobically illuminated cells. Figure 7, panel (g) shows, that 24 h after the illumination a smaller number of cells demonstrated morphological alterations, compared to cells illuminated under aerobic conditions (panel (e)). It was notable that shrunken, brightly stained nuclei, morphology typical for necrosis, were almost absent. Instead, fragmented, condensed chromatin granules characteristic of apoptosis (arrows) were apparent (Figure 7(g)). Figure 7, panels (h) and (j) demonstrate that cells illuminated under hypoxic conditions, but not treated with ZnTM-3-PyP, and cells treated with ZnTM-3-PyP in the dark, did not display morphological changes.

Discussion

The effect of PDT is manifested mainly through the induction of cell death. It has been reported that PDT can induce cell death by both apoptosis and necrosis [31,32]. Major factors that determine the type of PDT-mediated cell death include the light dose, subcellular distribution of the photosensitizer and the overall sensitivity of the cells [33,34]. Experiments with Photofrin have demonstrated that its subcellular localization determines distinct death phenotypes in response to PDT [32]. In this study cells were subjected to photosensitizer action in the presence of culture medium as an *in vitro* model of PDT activity. We have shown that the presence of oxygen during the illumination period is a critical factor that determines the type of cell death induced by ZnTM-3-PyP PDT. This supports the general idea that oxidative stress is the major cause of cancer cell damage induced by PDT. Photo-oxidative effects on the culture medium might also contribute to oxidative stress in this cell

culture model of PDT. The extent and nature of the oxidative injury determines whether the cell survives or undergoes apoptotic or necrotic death [3]. It is reasonable to expect that extensive oxidative damage leading to gross structural and/or metabolic alterations eventually causes necrotic death, while moderate oxidative damage could induce a death program, leading to apoptosis. This idea is consistent with our finding that illumination of ZnTM-3-PyP-treated cells in normal oxygen-containing atmosphere produces morphological changes typical for necrotic death, while illumination under hypoxic conditions produces changes that indicate apoptotic death.

We have shown that upon illumination ZnTM-3-PyP induces severe oxidative stress in LS147T colon adenocarcinoma cells. This is manifested by depletion of intracellular GSH, oxidative DNA damage and lipid peroxidation. Photo-inactivation of essential antioxidant enzymes such as glutathione reductase and glutathione peroxidase further exacerbates sensitivity to oxidative damage. Peroxidation of membrane lipids may itself be sufficient to cause cell death through an increase in plasma membrane permeability that depletes intracellular ATP [11], disrupts cell homeostasis and promotes the synthesis of stress-signalling molecules.

Further, we found that PDT with ZnTM-3-PyP causes a dramatic increase in 8-OHdG, which is produced as a consequence of oxidative DNA damage. Such DNA damage may by itself also be a sufficient reason for cell death.

Singlet oxygen is considered to be the main cause for 8-OHdG production in PDT. $^1O_2$ has a very short half-life, and migrates less than 0.02 μm in cells [35]; therefore the sites of photo-damage produced by this mechanism will correspond closely to the localization of the photosensitizer. Thus, it is likely that at least some ZnTM-3-PyP localizes in very close proximity to DNA.

In conclusion, photo-activation of ZnTM-3-PyP induces profound damage to the LS174T adenocarcinoma cells, manifested by inactivation of key antioxidant enzymes, peroxidation of membrane lipids leading to plasma membrane permeabilization, and oxidative DNA damage. Extensive oxidative injury seems to be a plausible explanation for ZnTM-3-PyP-induced necrotic cell death.

Acknowledgements

The authors thank Professor C. Ford from the Department of Surgery, Faculty of Medicine, Kuwait University, for providing the cell line used in this study and for his continuous support, and Dr M. Alkhalaf for the nuclei staining procedure. The excellent technical assistance of Fatima Sequeira is acknowledged. This work was supported by grant YM02/05 from Kuwait University. IBH acknowledges the support from NIH U19 AI67798-01 and Institute for the Study of Aging.

Note

‡M. Alkhalaf, Department of Biochemistry, Faculty of Medicine, Kuwait University—personal communication.

References

[1] Valko M, Morris H, Cronin MT. Metals, toxicity and oxidative stress. Curr Med Chem 2005;12:1161–1208.
[2] Halliwell B, Gutteridge JMC. Free radicals in biology and medicine. 3rd ed. New York, NY: Oxford University Press; 1999.
[3] Girotti AW, Kriska T. Role of lipid hydroperoxides in photo-oxidative stress signaling. Antioxid Redox Signal 2004;6: 301–310.
[4] Chatterjee SR, Srivastava TS, Kamat JP, Devasagayam TP. Lipid peroxidation induced by mesotetrakis[3,4-bis(carboxymethyleneoxy)phenyl] porphyrin on photosensitization in hepatic and tumor microsomes. Chem Biol Interact 1997;108: 27–37.
[5] Du HY, Olivo M, Tan BK, Bay BH. Hypericin-mediated photodynamic therapy induces lipid peroxidation and necrosis in nasopharyngeal cancer. Int J Oncol 2003;23:1401–1405.
[6] Geiger PG, Korytowski W, Lin F, Girotti AW. Lipid peroxidation in photodynamically stressed mammalian cells: Use of cholesterol hydroperoxides as mechanistic reporters. Free Radic Biol Med 1997;23:57–68.
[7] Wang HP, Qian SY, Schafer FQ, Domann FE, Oberley LW, Buettner GR. Phospholipid hydroperoxide glutathione peroxidase protects against singlet oxygen-induced cell damage of photodynamic therapy. Free Radic Biol Med 2001;30: 825–835.
[8] Nyman ES, Hynninen PH. Research advances in the use of tetrapyrrolic photosensitizers for photodynamic therapy. J Photochem Photobiol B-Biol 2004;73:1–28.
[9] Foote CS. Definition of type I and type II photosensitized oxidation. Photochem Photobiol 1991;54:659.
[10] Benov L, Batinic-Haberle I, Spasojevic I, Fridovich I. Isomeric *N*-alkylpyridylporphyrins and their Zn(II) complexes: Inactive as SOD mimics but powerful photosensitizers. Arch Biochem Biophys 2002;402:159–165.
[11] AlMutairi DA, Craik JD, Batinic-Haberle I, Benov LT. Photosensitizing action of isomeric zinc *N*-methylpyridyl porphyrins in human carcinoma cells. Free Radic Res 2006; 40:477–483.
[12] Dennis KJ, Shibamoto T. Gas chromatographic analysis of reactive carbonyl compounds formed from lipids upon UV-irradiation. Lipids 1990;25:460–464.
[13] Steghens JP, van Kappel AL, Denis I, Collombel C. Diaminonaphtalene, a new highly specific reagent for HPLC-UV measurement of total and free malondialdehyde in human plasma or serum. Free Radic Biol Med 2001;31: 242–249.
[14] Gardner PR. Aconitase: Sensitive target and measure of superoxide. Meth Enzymol 2002;349:9–23.
[15] Gardner PR, Nguyen DD, White CW. Aconitase is a sensitive and critical target of oxygen poisoning in cultured mammalian cells and in rat lungs. Proc Natl Acad Sci USA 1994;91: 12248–12252.
[16] McCord JM, Fridovich I. Superoxide dismutase. An enzymic function for erythrocuprein (hemocuprein). J Biol Chem 1969; 244:6049–6055.
[17] Visick JE, Clarke S. RpoS- and OxyR-independent induction of HPI catalase at stationary phase in *Escherichia coli* and

identification of rpoS mutations in common laboratory strains. J Bacteriol 1997;179:4158–4163.
[18] Smith IK, Vierheller TL, Thorne CA. Assay of glutathione reductase in crude tissue homogenates using 5,5′-dithiobis(2-nitrobenzoic acid). Anal Biochem 1988;175:408–413.
[19] Spector D, Goldman R, Leinwald L. Calls: A laboratory manual. Cold Spring Harbor, NY: Cold Spring Harbor Laboratory Press; 1997.
[20] Schafer FQ, Buettner GR. Redox environment of the cell as viewed through the redox state of the glutathione disulfide/glutathione couple. Free Radic Biol Med 2001;30:1191–1212.
[21] Griffith OW. Biologic and pharmacologic regulation of mammalian glutathione synthesis. Free Radic Biol Med 1999;27:922–935.
[22] Stark G. Functional consequences of oxidative membrane damage. J Membr Biol 2005;205:1–16.
[23] Niki E, Yoshida Y, Saito Y, Noguchi N. Lipid peroxidation: Mechanisms, inhibition, and biological effects. Biochem Biophys Res Commun 2005;338:668–676.
[24] Girotti AW. Lipid hydroperoxide generation, turnover, and effector action in biological systems. J Lipid Res 1998;39:1529–1542.
[25] Girotti AW. Photosensitized oxidation of membrane lipids: Reaction pathways, cytotoxic effects, and cytoprotective mechanisms. J Photochem Photobiol 2001;63:103–113.
[26] Inoue M, Sato EF, Nishikawa M, Park AM, Kira Y, Imada I, Utsumi K. Cross talk of nitric oxide, oxygen radicals, and superoxide dismutase regulates the energy metabolism and cell death and determines the fates of aerobic life. Antioxid Redox Signal 2003;5:475–484.
[27] Ochsner M. Photophysical and photobiological processes in the photodynamic therapy of tumours. J Photochem Photobiol B-Biol 1997;39:1–18.
[28] Phillipson RP, Tobi SE, Morris JA, McMillan TJ. UV-A induces persistent genomic instability in human keratinocytes through an oxidative stress mechanism. Free Radic Biol Med 2002;32:474–480.
[29] Oleinick NL, Morris RL, Belichenko I. The role of apoptosis in response to photodynamic therapy: What, where, why, and how. Photochem Photobiol Sci 2002;1:1–21.
[30] Kriska T, Korytowski W, Girotti AW. Hyperresistance to photosensitized lipid peroxidation and apoptotic killing in 5-aminolevulinate-treated tumor cells overexpressing mitochondrial GPX4. Free Radic Biol Med 2002;33:1389–1402.
[31] Agostinis P, Vantieghem A, Merlevede W, de Witte PA. Hypericin in cancer treatment: More light on the way. Int J Biochem Cell Biol 2002;34:221–241.
[32] Hsieh YJ, Wu CC, Chang CJ, Yu JS. Subcellular localization of photofrin determines the death phenotype of human epidermoid carcinoma A431 cells triggered by photodynamic therapy: When plasma membranes are the main targets. J Cell Physiol 2003;194:363–375.
[33] Dellinger M. Apoptosis or necrosis following photofrin photosensitization: Influence of the incubation protocol. Photochem Photobiol 1996;64:182–187.
[34] Kessel D, Luo Y, Deng Y, Chang CK. The role of subcellular localization in initiation of apoptosis by photodynamic therapy. Photochem Photobiol 1997;65:422–426.
[35] Moan J, Berg K. The photodegradation of porphyrins in cells can be used to estimate the lifetime of singlet oxygen. Photochem Photobiol 1991;53:549–553.